



Interpreting crosswell travelttime tomograms considering the available illumination

Renato R. S. Dantas* (PPGG/UFRN) and Walter E. Medeiros (DGEF/UFRN & CNPq/INCT-GP)

Copyright 2015, SBGf - Sociedade Brasileira de Geofísica

This paper was prepared for presentation at the 14th International Congress of the Brazilian Geophysical Society, held in Rio de Janeiro, Brazil, August 3-6 2015.

Contents of this paper were reviewed by the Technical Committee of the 14th International Congress of The Brazilian Geophysical Society and do not necessarily represent any position of the SBGf, its officers or members. Electronic reproduction or storage of any part of this paper for commercial purposes without the written consent of The Brazilian Geophysical Society is prohibited.

Abstract

The key aspect limiting resolution in crosswell travelttime tomography is illumination, a well known result but not as well exemplified. Resolution in the 2D case is revisited using a simple geometric approach based on the angular aperture distribution and the Radon Transform properties. It is revised the results that if an interface has dips contained in the angular aperture limits in all points, it is correctly imaged in the tomogram. In the inverse sense, however, if an interface is interpretable from a tomogram, even an approximately horizontal interface, there is no guarantee that it corresponds to a true interface. Interpretation must be done always taking in consideration the a priori information and the particular limitations due to illumination. An example of interpreting a real data survey in this context is also presented.

Introduction

Crosswell travelttime tomography is an important tool for characterizing aquifers and oil reservoirs (e.g. Harris et al., 1995; Day-Lewis and Lane, 2004; Plessix, 2006), and monitoring gas carbon sequestration in geologic formations (e.g. Ajo-Franklin et al., 2007; Ajo-Franklin, 2009; Byun et al., 2010). Obtained tomograms can also be used as starting models for more elaborated inversion methods, such as full waveform inversion (e.g. Wang and Rao, 2006; Virieux and Operto, 2009).

It is widely recognized (e.g. Menke, 1984; Rector III and Washbourne, 1994; Goudswaard et al., 1998; Day-Lewis and Lane, 2004) that in crosswell travelttime tomography it is difficult to reconstruct high-angle interfaces due to the absence of near-vertical rays. However, systematic approaches to investigate data resolution which might be easily adapted to particular designs are still necessary. Here, it is resumed the approach of using the angular aperture distribution, under the hypothesis that the interwell media is homogeneous (Rector III and Washbourne, 1994), now in concurrence with the Radon Transform properties (Menke, 1984; Kak and Slaney, 2001), to characterize data resolution in 2D crosswell travelttime tomography. Although both elements are valid only for the straight-ray case, they might constitute good approximations for the nonlinear case, at least when the slowness contrasts are smaller than 20% (Dines and Lytle, 1979; Bregman et al., 1989).

As result it is devised a framework to understand data resolution primarily based on simple geometric elements.

Tomography as an inverse problem

Travelttime tomography obtains images of the Earth's subsurface based on wave propagation between sources and receivers. Under the validity of the ray tracing approach (Cerveny, 2005), the travelttime τ between a source-receiver pair is given by

$$\tau(s) = \int_L s d\ell \quad (1)$$

where L is the ray path and $s = s(\ell)$ is the slowness along L .

Survey designs for geophysical applications usually impose limited illumination as consequence of positioning sources and receivers just in certain sectors of the \mathcal{R} boundary. In particular, for crosswell designs, sources and receivers can be placed just in the boreholes.

Here it is considered the 2-D discrete version of the P-wave crosswell tomography between two vertical boreholes. The slowness is defined by $s(x, z)$, where x and z axes coincide with the top horizontal and left vertical boundaries of the interwell region. This region is discretized in a rectangular mesh containing N ordered elements with sizes Δx and Δz . The associated slowness values s_j ($j = 1, 2, \dots, N$) are arranged in the vector array $\mathbf{s} \in \mathbb{R}^N$. In addition, the M available source-receiver pairs are ordered and the measured travelttimes t_i^{obs} ($i = 1, 2, \dots, M$) are arranged in the vector array $\mathbf{t}^{obs} \in \mathbb{R}^M$. Thus, the crosswell travelttime tomography problem can be formulated as

$$\mathbf{A}(\mathbf{s}) \cdot \mathbf{s} = \mathbf{t}^{mod} = \mathbf{t}^{obs} - \mathbf{n} \quad (2)$$

where $\mathbf{A} : \mathbb{R}^N \rightarrow \mathbb{R}^M$ is a matrix array whose i -th row approximates the ray path L (Equation 1) for the i -th source-receiver pair, and \mathbf{t}^{obs} is assumed to be the sum of \mathbf{t}^{mod} , the parcel that can be explained by the model, and \mathbf{n} , the remaining parcel or "noise".

In general \mathbf{A} depends on \mathbf{s} and Equation 2 is nonlinear. There are several modelling approaches to this equation (e.g. Vidale, 1988, 1990; Podvin and Lecomte, 1991; Moser, 1991). In this study, it is used the approach of Podvin and Lecomte (1991). If the slowness contrasts are smaller than 20% (Dines and Lytle, 1979; Bregman et al., 1989), the ray path can be approximated by just one straight line, \mathbf{A} is then constant and the inverse problem is linear. In this case, the crosswell tomography can be formulated as an incomplete Radon Transform (Kak and Slaney, 2001; Menke, 2012).

Estimating the slowness distribution using just the least-squares fitting of \mathbf{t}^{mod} and \mathbf{t}^{obs} in Equation 2 is an ill-posed

problem because its solution is neither unique nor stable. The classic approach to regularize this problem (Tikhonov and Arsenin, 1977) is to impose also the criteria of smooth variation of $s(x, z)$ (in the ℓ_2 norm):

$$\mathbf{s}^{est} = \arg \min_{\mathbf{s}} \{ \lambda \|\mathbf{D}\mathbf{s}\|_2^2 + \|\mathbf{A}\mathbf{s} - \mathbf{t}^{obs}\|_2^2 \} \quad (3)$$

where \mathbf{s}^{est} is an estimate of \mathbf{s} , λ is the Lagrange multiplier, and \mathbf{D} is the finite difference operator approximating the first or second order partial derivatives of $s(x, z)$. In general, a Lagrange multiplier should be chosen as the smallest value that still guarantees solution stability under noise variation (Tikhonov and Arsenin, 1977). Utilizing the smoothness constraint results in obtaining diffuse estimates for $s(x, z)$ usually lacking information on edge localization. This bias is intrinsically associated to the smoothness constraint.

Algorithms

In the linear case, it is used the Conjugate Gradient algorithm. This algorithm was initialized with a homogeneous media with slowness equal to the mean slowness. For the nonlinear case, it is used the Gauss-Newton-Marquardt method because of its fast convergence to a local minimum, given a feasible starting point. This point was chosen as the solution obtained with the linear approximation to \mathbf{A} . In all inversion examples to be presented, 30 iterations were sufficient to ensure convergence.

Resolution lack as result of limited illumination

The spatial variation of the angular aperture for an homogeneous media (Rector III and Washbourne, 1994) is shown in Figure (top). By dividing the interwell region in nine equal area sectors, a simplified version of this figure is shown as a diagram in Figure (bottom), where the angular aperture in each sector is taken approximately as the angular aperture at its centre. Based on the Fourier Slice Theorem for the Radon Transform (Kak and Slaney, 2001), this diagram shows, in each sector, the range of dips that an interface can take in order to be reconstructed.

Dantas and Medeiros (2015) concluded that if the interface dip is contained inside the angular aperture limits, it is correctly imaged in the tomogram. Unfortunately, the inverse is not true, that is, if an interface is interpretable from a tomogram, even an approximately horizontal interface, there is no guarantee that it corresponds to a true interface. In addition, interfaces can be only partially imaged. This result states the dilemma of ill-posed inverse problems. In the inverse sense, there is no guarantee of correspondence to the true distribution. Thus, interpreting crosswell tomograms is a task intrinsically different from interpreting complete illumination tomograms because there is no guarantee of correspondence to the true distribution, even if the interpreter confines himself/herself to interpret features that would have been hypothetically illuminated. Thus, interpretation must be done taking in consideration always both the limitations due to illumination and the available (or expected) geologic information. In fact, the interpreter usually interprets acceptable or expected features, even if he/she is not aware of this fact.

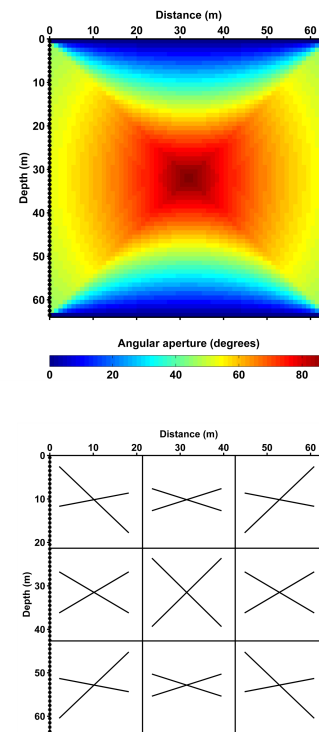


Figure 1: Angular aperture as function of position in a homogeneous media between two vertical boreholes (top) and its simplified version (bottom). Sources and receivers are shown in left and right boreholes, respectively. There are 64 equally spaced sources (or receivers). The interwell region was discretized with 64 x 64 equal area elements.

Application to real data

The ideas developed at Dantas and Medeiros (2015) are applied to the real data set available in the net as a tutorial test for the software Rayfract (Rayfract, 2014). These crosswell traveltime data result from a survey performed by the IGT (*International Geophysical Technology*) in an area of the Madrid-Barajas airport aiming to localize old galleries. The same data were utilized by Gholami and Siahkoohi (2010) for an inversion using joint sparsity constraints and by Göktürkler (2009) for an inversion using the smoothness constraint (1st order partial derivatives). Here, it is used the same discretization adopted by Gholami and Siahkoohi (2010) (128×64).

The available angular apertures (homogeneous media approximation, Rector III and Washbourne (1994)) are shown in Figure (left column). As consequence of a lower X/Z ratio, as compared with the design used in synthetic data (Figure), the angular aperture is 30% higher in the interwell central region. Tomogram obtained with smoothness constraint (Equation 3) is also shown in Figure (right column). The imaged features are similar to the ones obtained by both Gholami and Siahkoohi (2010) and Göktürkler (2009). The estimated background velocity (1.8 m/ms - 2.0 m/ms) is consistent with the expected velocity for saturated unconsolidated sandy-clay materials (Prasad et al., 2004), which can also be attributed to possibly existent saturated landfill material. Contrasting to this background, there are both negative (lower than

1.7 m/ms) and positive (higher than 2.1 m/ms) anomaly regions.

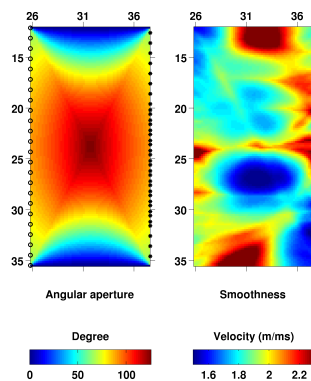


Figure 2: Real data - Madrid-Barajas airport experiment. Angular aperture as function of position in a homogeneous media (left) and tomogram resulting from nonlinear inversion using smoothness constraint (right, Equation 3).

Gholami and Siahkoohi (2010) highlighted the negative anomaly, with velocity around 1.5 m/ms, located in the interval depth 25 m - 28 m, interpreting it as water. This is a plausible interpretation given that the anomaly has shape compatible with a gallery and velocity value also compatible with an expected infilling of this gallery (water). The fact that this anomaly is positioned near the interwell central region, where the angular aperture is good, contributes to assign a relatively high confidence degree to this interpretation. Based on the expected rectangular shape for a gallery, one can even try to locate both their horizontal and vertical edges, and to interpret the positive anomaly above it as a thick horizontal cap, maybe a human construction. However, more caution should be taken when interpreting the positive anomalies localized in the top, bottom, and upper-right vertical boundaries. In the context, they possibly represent isolated blocks of rock or even pieces of human constructions. Nonetheless, it is difficult to interpret their shapes because of the low illumination.

Conclusion

The key limitation of crosswell tomography is illumination, a well known result but not as well stressed or exemplified. Because illumination is always incomplete, estimating the interwell velocity distribution from its tomogram is an ill-posed problem because even uniqueness is guaranteed. In this sense, interpreting crosswell tomograms is intrinsically different from interpreting tomograms resulting from complete illumination experiments. Taking an extrem case as the key example, even if the interpreted interface from a tomogram is approximately horizontal, there is no guarantee that it corresponds to a true interface that would be completely contained in the illumination limits. Thus, interpretation must be done taking in consideration both the available illumination and geologic information. Simple guides to survey design were also derived from the approach.

References

- Ajo-Franklin, J. B., 2009, Optimal experiment design for time-lapse traveltome tomography: *Geophysics*, **74**, Q27–Q40.
- Ajo-Franklin, J. B., B. J. Minsley, and T. M. Daley, 2007, Applying compactness constraints to differential traveltome tomography: *Geophysics*, **72**, R67–R75.
- Bregman, N., R. Bailey, and C. Chapman, 1989, Crosshole seismic tomography: *Geophysics*, **54**, 200–215.
- Byun, J., J. Yu, and S. J. Seol, 2010, Crosswell monitoring using virtual sources and horizontal wells: *Geophysics*, **75**, SA37–SA43.
- Dantas, R., and W. Medeiros, 2015, Resolution in crosswell traveltome tomography: the dependence from illumination. Submitted to *Geophysics*.
- Day-Lewis, F., and J. Lane, 2004, Assessing the resolution-dependent utility of tomograms for geostatistics: *Geophysical Research Letters*, **31**, no. 7, L07503.
- Dines, K. A., and R. J. Lytle, 1979, Computerized geophysical tomography: *Proceedings of the IEEE*, **67**, no. 7, 1065–1073.
- Gholami, A., and H. Siahkoohi, 2010, Regularization of linear and non-linear geophysical ill-posed problems with joint sparsity constraints: *Geophysical Journal International*, **180**, 871–882.
- Göktürkler, G., 2009, Seismic first-arrival tomography with functional description of traveltimes: *Journal of Geophysics and Engineering*, **6**, 374–385.
- Goudswaard, J. C., F. P. Ten Kroode, R. K. Snieder, and A. R. Verdel, 1998, Detection of lateral velocity contrasts by crosswell traveltome tomography: *Geophysics*, **63**, 523–533.
- Harris, J. M., R. C. Nolen-Hoeksema, R. T. Langan, M. Van Schaack, S. K. Lazaratos, and J. W. Rector III, 1995, High-resolution crosswell imaging of a west texas carbonate reservoir: Part 1-project summary and interpretation: *Geophysics*, **60**, 667–681.
- Kak, A. C., and M. Slaney, 2001, *Principles of computerized tomographic imaging*: Society for Industrial and Applied Mathematics.
- Menke, W., 1984, The resolving power of cross-borehole tomography: *Geophysical Research Letters*, **11**, 105–108.
- Plessix, R.-E., 2006, Estimation of velocity and attenuation coefficient maps from crosswell seismic data: *Geophysics*, **71**, S235–S240.
- Prasad, M., M. Zimmer, P. Berge, and B. Bonner, 2004, Laboratory measurements of velocity and attenuation in sediments: LLNL Rep. UCRL-JRNL, **205155**, 34.
- Rayfract, 2014, rayfract.com/tutorials, accessed 2014-07-07.
- Rector III, J. W., and J. K. Washbourne, 1994, Characterization of resolution and uniqueness in crosswell direct-arrival traveltome tomography using the fourier projection slice theorem: *Geophysics*, **59**, 1642–1649.
- Virieux, J., and S. Operto, 2009, An overview of full-waveform inversion in exploration geophysics: *Geophysics*, **74**, WCC1–WCC26.
- Wang, Y., and Y. Rao, 2006, Crosshole seismic waveform tomography-I. Strategy for real data application: *Geophysical Journal International*, **166**, 1224–1236.

Acknowledgments

CNPq is thanked for the MSc fellowship for RRS, the research fellowship and associated grant (Proc. 304301/2011-6) for WEM, and financial support by the

INCT-GP. The Podvin's algorithm and the data of the Madrid-Barajas experiment were downloaded from the net.